TEMPERATURE-DEPENDENT LIFETIME SPECTROSCOPY (TDLS) IN SILICON

S. Rein, T. Rehrl, W. Warta, and S.W. Glunz
Fraunhofer Institute for Solar Energy Systems (ISE), Heidenhofstr. 2, D-79110 Freiburg, Germany
Phone ++49 761-4588-5271; Fax ++49 761-4588-9000, e-mail: rein@ise.fhg.de

ABSTRACT: Carrier lifetime is very sensitive to electrically active defects. Apart from detecting the presence of recombination-active defects, lifetime measurements allow for a direct determination of defect parameters if the temperature or injection dependence of carrier lifetime is analyzed. The advantage of TDLS compared to other lifetime spectroscopic methods is that it allows a direct determination of the defect energy level E_t from the temperature dependence of LLI-SRH-lifetime measured on one single sample. As the accuracy of the E_t-determination strongly depends on the width of the temperature interval over which the characteristic Arrhenius-increase may be observed, different methods for an optimized data evaluation are proposed in the present work. Applying these new evaluation methods to TDLS-measurements taken on intentionally metal-contaminated silicon samples, excellent agreement between TDLS and DLTS is achieved. Thus, with these new data evaluation methods, TDLS allows for an accurate determination of the energy level E_t in a wide range of defect energies and doping concentrations. The main disadvantage of TDLS is its limited capability to resolve multiple active defect levels. In contrast to the prevalent interpretation of TDLS-data in literature, it is in no case possible to determine more than one defect level from fits to different linear regions in the Arrhenius-plot.

Keywords: Lifetime - 1: Spectroscopy - 2: Defects - 3.

1. INTRODUCTION

Since carrier lifetime is very sensitive to electrically active defects, lifetime measurements provide a powerful tool for defect characterization, even if the defect concentration is below the detection limit of deep-level transient spectroscopy (DLTS). Apart from detecting the presence of recombination-active defects, lifetime measurements allow for a direct determination of defect parameters if the temperature or injection dependence of carrier lifetime is analyzed [1,2]. The basic suitability of temperature-dependent lifetime spectroscopy (TDLS) for defect characterization has already been demonstrated theoretically and experimentally [3-5]. In this work advanced methods for the evaluation of TDLS-data are presented, which are increasing the accuracy of the determination of the defect level E_t. To validate the theoretical predictions, TDLS-measurements are performed on intentionally metal-contaminated samples using the microwave-detected photoconductance decay method (MW-PCD). Finally, the possibility to separate multiple defects by TDLS is discussed.

2. THEORY

Based on the Shockley-Read-Hall theory (SRH-theory) of carrier generation and recombination at a single defect level with energy E_t [6,7], the following well-known expression for the SRH-lifetime can be derived:

$$\tau_{SRH} = \frac{\tau_{n0}(p_0 + p_1 + \Delta n) + \tau_{p0}(n_0 + n_1 + \Delta n)}{p_0 + n_0 + \Delta n} \quad (1)$$

where n_o and p_0 are the thermal equilibrium concentrations of electrons and holes, respectively. As trapping is assumed to be negligible, the excess carrier concentrations of electrons and holes are equal ($\Delta n = \Delta p$). τ_{n0} and τ_{p0} are the capture time constants of electrons and holes which are proportional to the inverse product of the defect concentration N_t and the capture cross sections σ_n and σ_p for electrons and holes:

$$\tau_{p0} := \left[N_t \sigma_p v_{th}\right]^{-1} \quad \tau_{n0} := \left[N_t \sigma_n v_{th}\right]^{-1} \quad (2)$$

where v_{th} is the thermal velocity. The quantities n_1 and p_1 are given by the expression:

$$n_1 := N_C \exp\left(-\frac{E_C - E_t}{kT}\right) \quad p_1 := N_V \exp\left(-\frac{E_t - E_V}{kT}\right) \quad (3)$$

where E_t is the energy level of the recombination center, E_c and E_v are the energetic positions of the conduction and the valence band edge, and N_c and N_v are the effective state densities in the conduction and the valence band, respectively.

The general Eq. (1) is strongly simplified under LLI-conditions. Considering for example a defect level in the upper band gap in p-type silicon, the following equation can be derived:

$$\tau_{SRH}^{LLI}(T) = \tau_{n0}(T)\left[1 + k\frac{n_1(T)}{p_0}\right] \quad (4)$$

with a symmetry factor $k \equiv \tau_{p0}/\tau_{n0} = \sigma_n/\sigma_p$. The major contribution to the overall temperature dependence arises from the exponential temperature dependence of the SRH-density n_1. As n_1 depends on the density of states N_C, an additional temperature dependence of the form $N_C \propto T^{3/2}$ is superposed. Assuming that the capture cross sections σ_n, σ_p are temperature-independent, the capture time constant τ_{n0} only depends on temperature via the thermal velocity v_{th} leading to a temperature dependence of the form:

$$\tau_{n0}(T) = \left[N_t \sigma_n v_{th}(T)\right]^{-1} \propto T^{-1/2} \quad (5)$$

Restricting the analysis to the temperature range from 150 to ~500 K, the majority carrier concentration p_0 equals the doping concentration N_A and no temperature dependence has to be taken into account [8]. The upper temperature limit is slightly doping-dependent as it is given by the onset of intrinsic conduction (see below) [8].

To develop the overall temperature dependence, let us distinguish three temperature regions:

$$\begin{aligned} T \in T_{<} \quad & \text{such that} \quad n_1(T) << p_0 \\ T \in T_{trans} \quad & \text{such that} \quad n_1(T) \approx p_0 \\ T \in T_{>} \quad & \text{such that} \quad n_1(T) >> p_0 \end{aligned} \tag{6}$$

At sufficiently low temperatures ($T \in T_{<}$) the n_1/p_0-term in Eq. (4) can be neglected and the LLI-SRH-lifetime is given by $\tau_{n0}(T)$ with the temperature dependence of the thermal velocity indicated in Eq. (5).

At sufficiently high temperatures ($T \in T_{<}$) the defect-dependent n_1/p_0-term becomes dominant. By neglecting the τ_{n0}-term Eq. (4) approaches

$$\tau_{SRH}^{LLI}(T) = \tau_{n0}\, k\, \frac{n_1}{p_0} \;\propto\; T \exp\left(-\frac{E_C - E_t}{kT}\right) \tag{7}$$

In an Arrhenius-plot of the LLI-SRH-lifetime divided by temperature ($\ln(\tau(T)/T)$ vs. $1/T$), a linear increase is observed in the temperature range $T_{>}$:

$$\ln\left(\frac{\tau_{SRH}^{LLI}(T_>)}{T_>}\right) = -\frac{E_C - E_t}{kT_>} + const \tag{8}$$

As the slope in the Arrhenius-plot only depends on the energy level and is not influenced by other defect parameters, the defect energy may directly be extracted from a fit to the linear increase in the Arrhenius-plot.

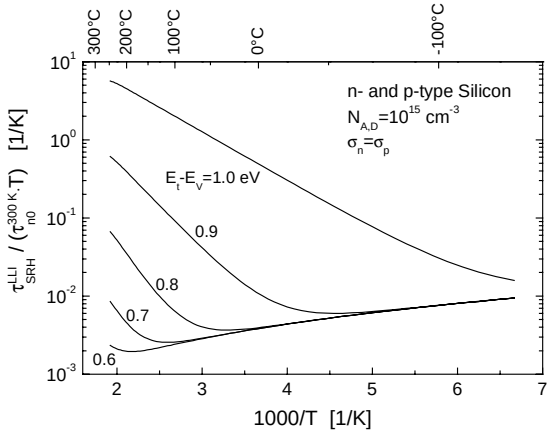

FIG. 1 Influence of the energy level E_t on the linear Arrhenius-increase of the temperature-dependent normalized LLI-SRH-lifetime.

Figure 1 shows the influence of the energy level on the overall temperature dependence of LLI-SRH-lifetime. The width of the temperature range, over which the characteristic Arrhenius-increase may be observed, strongly depends on energy level and doping concentration since the onset-temperature of the linear increase is shifted to higher values for deeper energy levels as well as higher doping concentrations. At high temperatures, the abrupt onset of intrinsic conduction leads to a strong lifetime decrease which completely screens the linear increase of the SRH-density (see Fig. 2). In the case of a 10^{15} cm^{-3} doped wafer an upper temperature limit of 500 K results for the evaluation of TDLS-data. For a 10^{14} cm^{-3} and a 10^{16} cm^{-3} doped wafer this intrinsic upper limit is shifted to 420 K and to 580 K, respectively. Thus, especially for highly doped samples or defect levels close to mid-gap, the temperature range exhibiting the linear increase may be reduced to such an extent that an accurate determination of the energy level is no longer possible.

3. PROBLEMS OF THE SIMPLE DATA EVALUATION AND ADVANCED METHODS

3.1 Linearized data evaluation

In order to extend the applicability of TDLS, Ling and Cheng [9] proposed a procedure to expand the temperature range of the linear increase based on a 'linearization' of the transition region. As the $\tau_{n0}(T)$-term in Eq. (4) cannot be neglected for $T \in T_{trans}$, they proposed to define a modified lifetime $\tau^*(T)$ by subtracting $\tau_{n0}(T)$ from the measured lifetime. As the LLI-SRH-lifetime measured at a temperature $T_L \in T_{<}$ equals $\tau_{n0}(T_L)$, they propose to determine $\tau_{n0}(T)$ by the following expression:

$$\tau_{n0}^*(T, T_L) = \tau_{n0}(T_L)\left(\frac{T}{T_L}\right)^{-0.5} = \tau_{SRH}^{LLI}(T_L)\left(\frac{T}{T_L}\right)^{-0.5} \tag{9}$$

With the modified lifetime $\tau^*(T)$:

$$\tau^*(T) := \tau_{SRH}^{LLI}(T) - \tau_{n0}^*(T, T_L) \tag{10}$$

the energy level is then extracted from a plot $\ln(\tau^*(T)/T)$ vs. $1/T$.

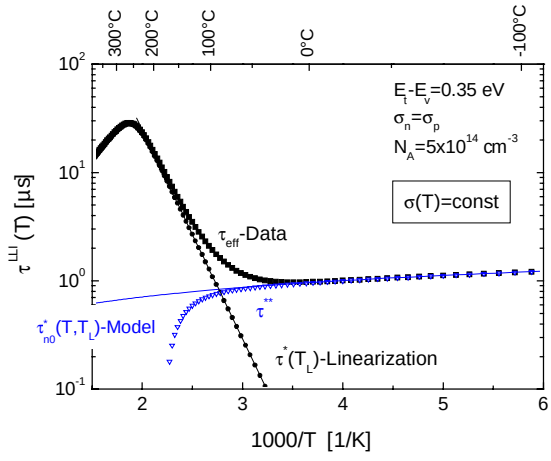

FIG. 2 Linearization of the transition region according to the procedure proposed in Ref. 9 demonstrated for a simulated data set. The abrupt strong lifetime decrease for high temperatures is due to intrinsic conduction.

The benefit of this evaluation is demonstrated in Fig. 2 on a simulated data set: while the temperature region of the

linear Arrhenius-increase is narrow for the raw data, it is strongly extended for the $\tau^*(T)$ data, which might significantly increase the accuracy of a fit in an experiment. A fundamental prerequisite for the accuracy of this linearization is that the temperature dependence of LLI-SRH-lifetime measured for $T \in T_<$ can be simulated by Eq. (9). Unfortunately, under realistic circumstances this is often *not* the case. The observed deviations most likely result from a temperature dependence of the capture cross section that is not considered by the modeling in Eq. (9).

Linearizing such 'non-ideal' but realistic TDLS-curves according to Eq. (9) and (10) leads to $\tau^*(T)$-curves that strongly depend on the *choice of* T_L. This problem is simulated in Fig. 3 for a defect level with a capture cross section that increases exponentially with increasing temperature as it is typical for multiphonon-capture. For comparison, the ideal data linearization labeled $\tau^{***}(T)$ which is discussed below is plotted as well (solid circles). It becomes obvious that the deviation of the $\tau^*(T)$-curve from the ideal $\tau^{***}(T)$-curve increases with decreasing T_L.

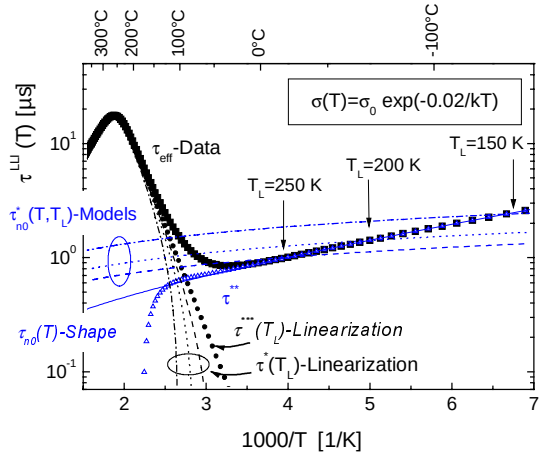

FIG. 3 Linearization of the transition region for a simulated dataset assuming a defect with temperature-dependent capture cross section: The quality of the procedure proposed in Ref. 9 (lines) strongly depends on the reference temperature T_L. For comparison, the new, optimized procedure proposed in this work is displayed (solid circles).

3.2 Optimized data linearization

In order to minimize or even eliminate these evaluation errors in the case of an additional temperature dependence for $T \in T_<$, we propose three advanced procedures for data evaluation.

The first procedure aims at an optimization of the T_L-determination while the linearization model itself remains unchanged. On the one hand T_L has to be chosen low enough that the corresponding lifetime is not yet influenced by the linear increase. On the other hand T_L has to be chosen close to the transition region T_{trans}, in order to avoid a distortion of the $\tau^*(T)$-curve due to deviations between the modeled and the measured τ_{n0}-dependence. Thus, the optimum T_L is the upper limit of the $T_<$-region.

To be able to determine this optimum T_L, an auxiliary function $\tau^{**}(T)$ is defined from the measured data which approximate the *real* temperature dependence of τ_{n0} in the whole temperature range: Analog to Eq. (9) the temperature dependence of the term $k\tau_{n0}n_1/p_0$ in Eq. (4) may be modeled using a lifetime value measured at a temperature T_H within the exponential regime ($T_H \in T_>$) if the temperature dependence given in Eq. (7) is taken into account:

$$\tau_{\substack{Exp \\ Term}}(T;T_H) = \tau_{SRH}^{LLI}(T_H)\frac{T}{T_H}\exp\left(-\frac{\Delta E_t}{k}\left(\frac{1}{T}-\frac{1}{T_H}\right)\right) \quad (11)$$

The auxiliary function $\tau^{**}(T)$:

$$\tau^{**}(T) = \tau_{SRH}^{LLI}(T) - \tau_{ExpTerm}(T;...) \quad (12)$$

then incorporates the complete temperature dependence of τ_{n0} (see open triangles in Fig. 2 and Fig. 3). Thus, the optimum T_L lies at that temperature, where the measured lifetime curve starts deviating from the $\tau^{**}(T)$-curve. As $\tau^{**}(T)$ depends on the value of ΔE_t yet to be determined, an iterative procedure has to be used: ΔE_t and $T_H \in T_>$ (from original data) $\rightarrow$ $\tau^{**}(T)$ $\rightarrow$ T_L-optimum $\rightarrow$ $\tau^*(T)$ $\rightarrow$ ΔE_t (from linearized data) $\rightarrow$ ... . Usually, a self-consistent solution is achieved after 2-3 runs.

An alternative advanced procedure of data evaluation leads to the $\tau^{***}(T)$-curve in Fig. 3. The procedure is similar to the one given by Eq. (9) and (10) with two important changes: First, the actually measured temperature dependence of τ_{n0} is modeled including a suitable model $\sigma(T)$ for the capture cross section. The linearization is achieved as before by subtracting the modeled $\tau_{n0}(T,T_L)$ from the measured data. It should be emphasized that due to the correct consideration of the measured $\tau_{n0}(T)$, $\tau^{***}(T)$ does not depend on the choice of T_L. The second difference to the standard procedure is, that $\tau^{***}(T)$ has to be divided by $T/\sigma(T)$ in order to allow a correct determination of ΔE_t from an Arrhenius-plot.

As the third and the last of the advanced procedure of data evaluation the fitting of the complete TDLS-curve should be mentioned.

3.3 Experimental Results

In order to demonstrate the influence of the improved data evaluation on the TDLS-results, we performed TDLS-measurements on different p-type silicon samples that were intentionally contaminated with different metals during crystal growth. While the defect concentration indicated in the following figures is calculated from the metal quantity added to the melt, the doping concentrations are measured by the 4-point-probe technique. In order to minimize the surface recombination, the samples were first damage-etched in an acid etch and then coated on both sides with silicon nitride leading to surface recombination velocities below 20 cm/s in the whole injection range [10]. The TDLS-measurements are performed by means of the

contactless microwave-detected photoconductance decay (MW-PCD) method (for details of the experimental setup see Ref. 5). To guarantee low injection conditions, the life-time measurements were performed at the minimum bias light intensity excluding trapping effects (for details see Ref. 2)

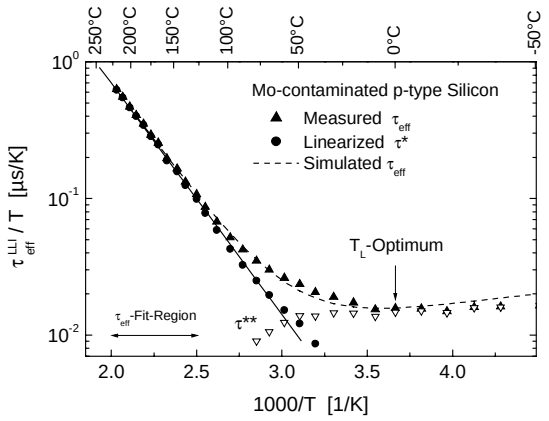

FIG. 4 TDLS-curve measured on an intentionally molybdenum-contaminated p-type silicon sample ([Mo] = 3.7×10^{11} cm^{-3}, $N_A = 9.9\times10^{14}$ cm^{-3}). Application of different data evaluation techniques (see text).

Figure 4 shows a TDLS-curve measured on a Mo-contaminated sample. The energy level ΔE_t is extracted by each of the methods discussed above. As the linear Arrhenius-increase is observed over a broad temperature range, only slight variations of ΔE_t are found for the different methods: (i) $\Delta E_t = 0.329 \pm 0.003$ eV from a linear fit (400-500 K) to the Arrhenius-increase of the measured lifetimes $\tau_{eff}(T)$, (ii) $\Delta E_t = 0.336 \pm 0.003$ eV from a linear fit (330-500 K) to the Arrhenius-increase of the linearized lifetimes $\tau^*(T)$ (solid line) and (iii) $\Delta E_t = 0.335 \pm 0.005$ eV from a fit to the entire TDLS-curve according to Eq. (4) (220-500 K) (dashed line). In literature [11] two molybdenum donor levels have been determined from DLTS-measurements: one at E_C-0.33 eV and another at E_V+0.34 eV. This shows the excellent agreement between TDLS and DLTS.

For the TDLS-curve displayed in Fig. 5, which was measured on a Ti-contaminated sample, the linear range in the Arrhenius-plotis strongly reduced due to the onset of intrinsic conduction. If the linear increase of the measured data is evaluated directly, an energy level $\Delta E_t = 0.181$ eV is found which does not agree with DLTS-values reported in literature. In contrast, the evaluation of the linearized data $\tau^*(T)$ using the optimum T_L as described above leads to a deeper defect level at $\Delta E_t = 0.242$ eV, which was confirmed by standard DLTS on a neighbouring sample ($E_C - E_t = 0.244$ eV) in agreement with the literature value of $E_C - E_t = 0.240$ eV [12]. The excellent agreement with DLTS compared to the uncertainty in the previous evaluation demonstrated in Fig. 3 proves the accuracy of the optimized linearization procedure.

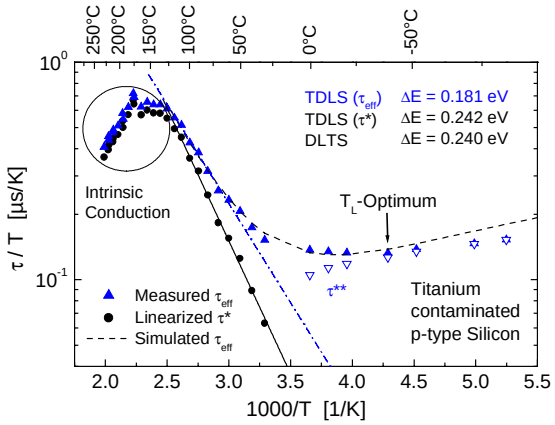

FIG. 5 TDLS-curve measured on an intentionally titanium-contaminated p-type silicon sample ([Ti] = 5.1×10^{12} cm^{-3}, $N_A = 4.6\times10^{14}$ cm^{-3}). Application of different data evaluation techniques (see text).

4. RESOLUTION CAPABILITY

Finally, the possibility to separate multiple defects by TDLS will be discussed. Fig. 6 shows as an example the TDLS-curve measured on an intentionally cobalt-contaminated sample. The simulation of the entire TDLS curve reveals that the measured temperature dependence cannot be simulated with one single defect level even if a temperature-dependent capture cross section is assumed. This strongly indicates the superposition of a second defect level. As a two-defect-simulation of a TDLS-curve (with 6 free parameters) is not unambiguous, we tried to simulate the measured TDLS-curve with two known cobalt levels reported in literature [13]: $E_C - E_{tA} = 0.41$ eV and $E_C - E_{tB} = 0.21$ eV. Assuming a slight temperature-dependence for the capture cross section of the shallower defect B, good agreement between the measured and the simulated curve can be achieved (see Fig. 6). Ling et al. [9] stressed that a linearization of TDLS-data may allow the extraction of multiple defect levels from linear fits in different temperature regions. The attempt to determine E_{tA} and E_{tB} in the above example from a fit to the two linear regions exhibited at 440-500 K and at 300-380 K led to energy levels $\Delta E_{t1} = 0.25 \ldots 0.29$ eV and $\Delta E_{t2} = 0.06 \ldots 0.10$ eV, respectively, depending on the evaluation procedure and the exact temperature region. The reason for the strong deviation from the theoretical values is due to the fact that especially the data within 300-380 K are strongly influenced by defect A *and* B, which does not allow the determination of the energy level of defect B.

From a more detailed analysis it is concluded that in contrast to the prevalent interpretation of TDLS-curves in literature [9], it is *never* possible to determine more than one defect level from fits to different linear regions, if LLI-

SRH-lifetime is influenced by more than one defect. TDLS-measurements only allow the determination of the defect level E_{tA} with highest recombination activity. The detailed analysis shows that for multiple defects the accuracy of the E_{tA}-determination strongly depends (i) on the difference E_{tA}-E_{tB} between the energy levels of the two defects and (ii) on the ratio $\sigma_{nB}N_{tB}/\sigma_{nA}N_{tA}$ of the 'effective' capture capture cross section of the two defects. While the energy difference determines the horizontal shift of the slopes in an Arrhenius-plot, the $\sigma_n N_t$-ratio determines the vertical shift of the entire TDLS curves since the $\sigma_n N_t$-product is a measure of the overall recombination activity of a defect.

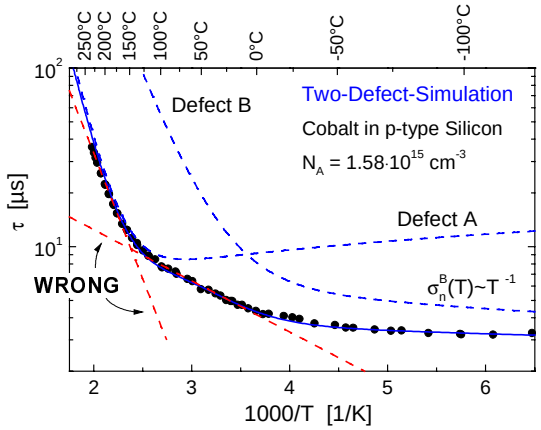

FIG. 6 TDLS-curve measured on an intentionally cobalt-contaminated p-type silicon sample ([Co] = 2.9×10^{14} cm^{-3}, $N_A = 1.58\times10^{15}$ cm^{-3}). Simulation of the entire TDLS-curve requires two defect levels (see text). An evaluation of the two linear regions does *not* allow a separation of the two defect levels.

5. CONCLUSION

The advantage of TDLS compared to other lifetime spectroscopic methods is that it allows a direct determination of the defect energy level E_t from the temperature dependence of LLI-SRH-lifetime measured on one single sample. As the accuracy of the E_t-determination strongly depends on the width of the temperature interval, over which the characteristic Arrhenius-increase may be observed, we propose different methods for an optimized data evaluation. Applying these new evaluation methods to TDLS-measurements taken on intentionally metal-contaminated silicon samples, excellent agreement between TDLS and DLTS could be achieved. Thus, with these new data evaluation methods, TDLS can be applied with high accuracy in a strongly extended range of defect energies and doping concentrations.

The main disadvantage of TDLS is its limited capability to resolve multiple active defect levels. It is shown that TDLS-measurements only allow the determination of the defect level with highest recombination activity. In contrast to the prevalent interpretation of TDLS-data in literature, it is *never* possible to determine more than one defect level from fits to different linear regions in the Arrhenius-plot.

ACKNOWLEDGEMENTS

The authors would like to thank H. Lautenschlager, T. Leimenstoll, M. Kwiatkowska and C. Schetter for sample preparation, S. Kaufmann and E. Tavaszi for important measurements and E. Schäffer for editorial support. This work was supported by the German Ministry of Education and Research BMBF (contract number 01SF0010).

REFERENCES

[1] W. M. Bullis and H. R. Huff, J. Electrochem. Soc. **143,** 1399-405 (1996).

[2] S. Rein, T. Rehrl, W. Warta, and S. W. Glunz, accepted for publ. in J. Appl. Phys. (2001).

[3] F. Shimura, T. Okui, and T. Kusama, J. Appl. Phys. **67,** 7168-71 (1990).

[4] Y. Kirino, A. Buczkowski, Z. J. Radzimski, G. A. Rozgonyi, and F. Shimura, Appl. Phys. Lett. **57,** 2832-4 (1990).

[5] S. Rein, T. Rehrl, J. Isenberg, W. Warta, and S. W. Glunz, *Proc. 16th EC-PVSEC* (Glasgow, UK, 2000), p. 1476-81.

[6] W. Shockley and W. T. Read, Phys. Rev. **87,** 835 (1952).

[7] R. N. Hall, Phys. Rev. **87,** 387 (1952).

[8] S. M. Sze, *Physics of Semiconductor Devices*, 2nd ed. (John Wiley & Sons, New York, 1981).

[9] C. H. Ling and Z. Y. Cheng, Appl. Phys. Lett. **71,** 3218-20 (1997).

[10] H. Maeckel and R. Luedemann, to be published (2001).

[11] L. Börnstein, *Semiconductors*, Vol. 17 (Springer-Verlag, Berlin, 1984).

[12] A. M. Salama and L. J. Cheng, J. Electrochem. Soc. **127,** 1164-7 (1980).

[13] K. Graff, *Metal Impurities in Silicon-Device Fabrication*, 1st ed. (Springer-Verlag, Berlin, 1995).

6. ADDITIONAL INFORMATION

3.4 Theorie

Include intrinsic conduction in the exemplary plots

Combined plot showing Et and NA influence

3.5 Advanced linearization

Add a **flow-diagram** in the journal paper.

3.6 Eperiment (Long introduction including all details of the experiment)

In order to demonstrate the influence of the improved data evaluation on the TDLS-results, we performed TDLS-measurements on different p-type silicon samples that were intentionally contaminated with different metals during crystal growth. While the defect concentration indicated in the following figures are calculated from the metal quantity added to the melt, the doping concentrations are measured by 4-point-probe technique.

In order to minimize the surface recombination, the sample were first damage-etched in an acid etch (CP133). Then both surfaces of the samples were coated with silicon nitride deposited in a PECVD-system at 375°C. After a final annealing step at 425°C for 25 min, this surface passivation is leading to surface recombination velocities below 20 cm/s in the whole injection range from 10^{12} to 10^{16} cm^{-3} [10].

The TDLS-measurements are performed by means of the contactless microwave-detected photoconductance decay (MW-PCD) method [14,15]. A liquid nitrogen cooled cryostat is integrated in the MW-PCD-system allowing lifetime measurements in a temperature range from 77 K to 500 K (for details see Ref. 32). In order to guarantee a precise temperature control, the temperature is measured directly on the sample surface with a Pt100 temperature sensor.

For TDLS-measurements as exemplified in Fig. 4, the adjustment of LLI-conditions for the lifetime measurements can be a crucial point. At very low injection densities (around 10^{13} cm^{-3}), the measured carrier lifetime of most samples shows a strong increase with decreasing excess carrier concentration. This behavior can be attributed to a carrier trapping effect [16]. As trapping effects screen the studied recombination properties of the defects, they have to be excluded. Thus, the determination of carrier lifetime for the TDLS curve requires at each temperature a variation of the bias light at low intensities. If the constant lifetime region expected from theory is not observed, the lifetime minimum is identified with the LLI-SRH-lifetime.

3.7 Molybdenum (Mo1) (JAP-discussion about k-determination)

The resulting TDLS-curve . From a fit to the linear increase above 110°C (solid line) an energy level of 0.330 eV is determined. This value is well confirmed by a fit to the entire TDLS-curve (dashed line) leading to an energy level of 0.335 eV. Both values correspond very well with the values reported in literature where two molybdenum donor levels have been determined from DLTS-measurements: the first one at 0.33 eV below the conduction band and the second one at 0.34 eV above the valence band [11]. As the linear increase produced by n_1 and p_1 is identical for the same ΔE, a fit to the linear increase does not reveal whether the defect level lies in the upper or the lower half of the band gap. Only a fit to the entire TDLS-curve allows for this information. From the fact that the TDLS-curve of the molybdenum sample *cannot* be simulated for a defect level at 0.335 eV *above the valance band* it can be concluded that the observed level lies in the upper half of the band gap. The best fit result (dashed line in Fig. 13) is achieved for a defect center with E_C-E_t = 0.335 eV, k = 4.55 and τ_{n0}(262K) = 4.09 µs. The excellent agreement between TDLS and DLTS concerning the position and depth of the defect shows the potential of TDLS. The circumstances under which an entire TDLS-fit allows for an unambiguous determination of the symmetry factor k – as for the present sample – and the problems associated with an entire TDLS-fit will be discussed in detail elsewhere.

3.8 Titanium

New data evaluation, ...

... Extracting errors for the energy levels.

... checking the quality of DLTS-result.

3.9 Cobalt (One-and-Tow-Defect-Simulation)

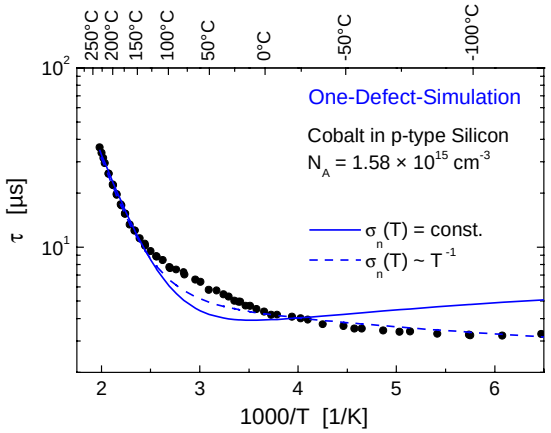

FIG. 7